# Enantiopure Siloxy-Functionalized Group 4 Metallocene Dichlorides. Synthesis, Characterization, and Catalytic Dehydropolymerization of $PhSiH_3$

Brian J. Grimmond,[1,†] Nigam P. Rath, and Joyce Y. Corey*

*Department of Chemistry, University of Missouri−St. Louis, 8001 Natural Bridge Road, St. Louis, Missouri 63121*

*Received April 7, 2000*

A series of chiral enantiopure group 4 metallocene dichlorides $(Cp^{Si*})_2MCl_2$ [$Cp^{Si*} = \eta^5$-$C_5H_4SiMe_2$(**1***R*)-*endo*-(+)-$OC_{10}H_{17}$, M = Zr, **3**; Hf, **4**] and $Cp(Cp^{Si*})MCl_2$ [Cp = $\eta^5$-$C_5H_5$, M = Ti, **5**; Zr, **6**] were synthesized as precatalysts for the dehydropolymerization of $PhSiH_3$. The time-averaged $C_2$-symmetric metallocene dichlorides $(Cp^{Si*})_2MCl_2$ (M = Zr, Hf) were prepared by the metathesis reaction of 2 equiv of $(Cp^{Si*})$Li, **2**, with the appropriate metal tetrachloride $MCl_4$·2THF. The $C_1$-symmetric compounds $Cp(Cp^{Si*})MCl_2$ (M = Ti, Zr) were synthesized by a similar metathesis reaction of $(Cp^{Si*})$Li and the precursor $CpMCl_3$ (M = Ti, Zr·2THF). All compounds were characterized by elemental analysis and $^1H$, $^{13}C\{^1H\}$, and $^{29}Si\{^1H\}$ NMR spectroscopy in addition to various 2D NMR spectroscopy techniques. A crystalline sample of **6** was studied by X-ray diffraction, which confirmed the pseudo-tetrahedral geometry of the Zr metal center and the $C_1$ symmetry of the overall complex. A 1.0 mol % loading of the chiral precatalysts **3**−**6** was combined with 2.0 mol % of *n*-BuLi to provide an in situ catalyst for the dehydropolymerization of $PhSiH_3$ to polyphenylsilane. The performance of each chiral catalyst was assayed with respect to polymer molecular weight properties and polymer microstructure. Substituted zirconocenes **3** and **6** were found to produce higher average molecular weight polymers ($M_w$ = 4100) by GPC analysis. The characterization of each by $^{29}Si\{^1H\}$ NMR spectroscopy indicated that all polyphenysilanes consisted of atactic microstructures (mm = 0.20, mr = 0.50, rr = 0.30).



## Introduction

Polysilanes are a relatively new class of inorganic polymers with numerous potential applications.[2] The physical characteristics of polysilanes and polymers in general depend on the average molecular weight properties. In the case of polymers containing stereogenic centers, the degree of stereoregulation of the polymer chain or network can also define numerous physical characteristics.[3] Therefore, by controlling the macromolecular properties of a particular polymer, it is possible to construct new polymers with various desirable physical features. Focusing on the synthesis of unsymmetrical polysilanes in a sterocontrolled manner, the popular method of Wurtz-type coupling of prochiral organochlorosilanes has resulted in the production of polymers containing some degree of stereobias.[4] However, the reliable production of highly stereoregular polysilanes (meso replication probability (Pm) > 0.95) by this method has not yet been achieved.

There are several alternative approaches to the synthesis of polysilanes, perhaps the most attractive of which is that of the catalytic dehydrocoupling of primary silanes.[5] Group 4 metallocene systems have been used as catalysts for the production of highly stereoregular isotactic and syndiotactic polyolefins.[6] The nature of the polyolefin obtained can be precisely controlled by the structure of the catalyst, the cocatalyst, and the general experimental conditions used. It would therefore seem reasonable that a similar approach to the synthesis of polysilanes could potentially produce stereoregular polysilanes. Group 4 metallocene dichlorides in combination with a cocatalyst such as *n*-BuLi are commonly used as dehydropolymerization catalysts, although various other catalyst systems have also been investigated.[7] The dehydropolymerization of monomers such as $PhSiH_3$ can produce polyphenylsilanes (PPSi) with atactic (*a*-PPSi), isotactic (*i*-PPSi), or syndiotactic (*s*-PPSi) stereoarrangements. We have recently investi-

* To whom correspondence should be addressed. E-mail: corey@jinx.umsl.edu.
† Present address: Department of Chemistry, Yale University, New Haven, CT 06520. E-mail: brian@jaxindy.chem.yale.edu.

(1) Taken from the Ph.D. Thesis of Brian J. Grimmond, University of Missouri−St. Louis, 1999.

(2) (a) West, R. *J. Organomet. Chem*. **1986**, *300*, 327. (b) Miller, R. D.; Michl, J. *Chem. Rev*. **1989**, *89*, 1359.

(3) Hauptmann, E.; Waymouth, R. M.; Ziller, J. W. *J. Am. Chem. Soc.* **1997**, *119*, 11174.

(4) (a) Jones, R. G.; Benfield, R. E.; Evans, P. J.; Holder, S. J.; Locke, J. A. M. *J. Organomet. Chem*. **1996**, *521*, 171. (b) Maxka, J.; Mitter, F.; Powell, D. R.; West, R. *Organometallics* **1991**, *10*, 660. (c) Wolff, A. R.; Nozue, I. Maxka, J.; West, R. *J. Polym. Sci., Part A: Polym. Chem*. **1988**, *26*, 701.

(5) (a) Tilley, T. D. *Acc. Chem. Res*. **1993**, *26*, 22. (b) Harrod, J. F. *Prog. Catal*. **1992**, 147. (c) Corey, J. Y. In *Advances in Silicon Chemistry*; Larson, G., Ed.; JAI Press: Greenwich, CT, 1991; Vol. 1, p 327.

(6) Brintzinger, H. H.; Fischer, D.; Mülhaupt, R.; Rieger, B.; Waymouth, R. M. *Angew. Chem., Int. Ed. Eng*. **1995**, *34*, 1143.

(7) (a) Fontaine, F. G.; Kadkhodazadeh, T.; Zargarian, D. *Chem. Commun*. **1998**, 1253- 1254. (b) Yang, S. Y.; Park, J. M.; Woo, H. G.; Kim, W. G.; Kim, I. S.; Kim, D. P.; Hwang, T. S. *Bull. Korean Chem. Soc.* **1997**, *18*, 1264 (*CA*).

10.1021/om0002935 CCC: $19.00 
Publication on Web 06/30/2000

gated the ability of a homologous series of substituted group 4 metallocene dichlorides in combination with 2 *n*-BuLi as dehydropolymerization catalysts for $PhSiH_3$.[8] The PPSi polymerisates obtained were characterized with respect to the molecular weight properties and microstructure. It was concluded that, generally, the choice of catalyst influenced the degree of $PhSiH_3$ polymerization, with substituted zirconocenes producing PPSi samples of the highest $M_w$. However, the entire range of achiral catalysts studied were consistently found to produce *a*-PPSi as established by $^{29}Si\{^1H\}$ NMR spectroscopy.[9,10] This report describes our attempts to produce stereoregular PPSi via an enantiomorphic site control mechanism by using the new enantiopure metallocene dichlorides $(Cp^{Si*})_2MCl_2$ [$Cp^{Si*} = \eta^5$-$C_5H_4SiMe_2$(1*R*)-*endo*-(+)-$OC_{10}H_{17}$, M = Zr, Hf] and $Cp(Cp^{Si*})MCl_2$ [Cp = $\eta^5$-$C_5H_5$, M = Ti, Zr].

## Results

**Metallocene Syntheses and Characterization.** The series of asymmetric siloxy-functionalized metallocene dichlorides were synthesized from the known precursor $C_5H_5SiMe_2$(1*R*)-*endo*-(+)-$OC_{10}H_{17}$, **1**.[11] Deprotonation of an $Et_2O$ solution of **1** with *n*-BuLi resulted in the precipitation of the corresponding lithium salt $LiC_5H_4SiMe_2$(1*R*)-*endo*-(+)-$OC_{10}H_{17}$, **2** (eq 1), as a moisture sensitive, white powder. The use of alternative solvents such as pentanes or THF provided **2** in lower yield.

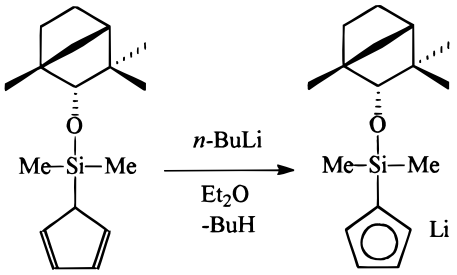


(1)

The $C_2$-symmetric heteroannular disubstituted zirconocene $(Cp^{Si*})_2ZrCl_2$, **3**, was synthesized from $ZrCl_4$·2THF and 2 equiv of **2** in toluene (eq 2). Filtration of

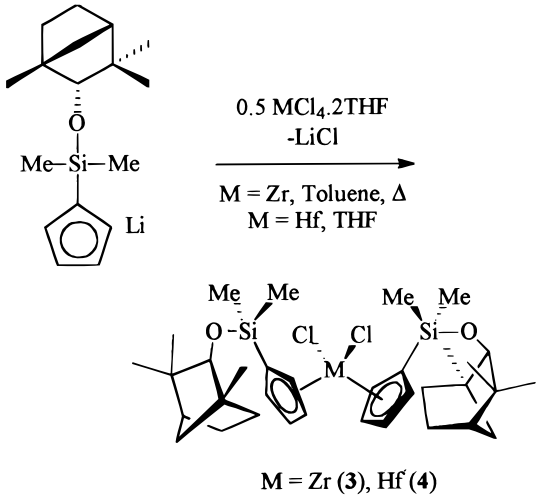


(2)

M = Zr (**3**), Hf (**4**)

the reaction mixture through Celite afforded a clear yellow solution. After removal of the solvent a solid was obtained, which was sublimed to provide analytically pure **3** as a white solid in reasonable yield (60%). The hafnium analogue, **4**, was obtained from $HfCl_4$·2THF and 2 equiv of **2** in THF at ambient temperature. The solid obtained after removal of the solvent was recrystallized from $CH_2Cl_2$/pentane to give analytically pure **4** as a white powder in 12% yield. Attempts to synthesize the corresponding titanocene by several methods failed. The characterization of compounds **3** and **4** by $^1H$, $^{13}C\{^1H\}$, and $^{29}Si\{^1H\}$ NMR spectroscopy suggested that the metallocene dichlorides existed in solution with time-averaged $C_2$ symmetry.[10a,12] The $^1H$ NMR spectrum ($CDCl_3$) of **3** shown in Figure 1 exhibits four resonances in the cyclopentadienyl region for the four individual protons on each of the equivalent $Cp^{Si*}$ rings. The coupling constant between the Cp protons ($J$ = 2.6 Hz) was typical for monosubstituted cyclopentadienyl rings of group 4 metallocene dichlorides. Two diastereotopic $SiMe_2$ singlets and one collection of fenchoxy resonances were observed, consistent with the presence of a single $Cp^{Si*}$ ring environment. The presence of one type of fenchoxy ligand was most reliably indicated by the three singlets, each of relative intensity three (Figure 1). These signals represented the three inequivalent methyl groups of the fenchoxy substituent. The $^{13}C\{^1H\}$ NMR spectrum displayed 17 signals associated with the total number of inequivalent $^{13}C$ nuclei present within the $Cp^{Si*}$ ancillary ligand.[13] Finally, one singlet was obtained in the $^{29}Si\{^1H\}$ NMR spectrum, indicating the

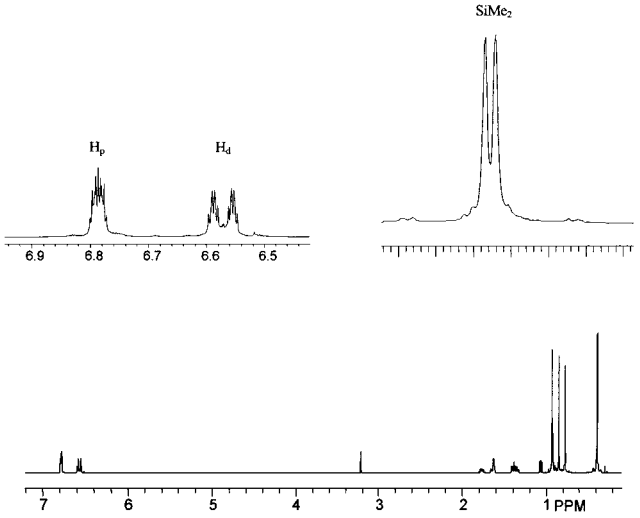


**Figure 1.** $^1H$ NMR spectrum ($CDCl_3$, 500 MHz) of $(Cp^{Si*})_2ZrCl_2$, **3**. The insets display the proximal ($H_p$) and distal ($H_d$) cyclopentadienyl protons and the diastereotopic $SiMe_2$ groups. The insets are not set to scale.

(8) (a) Grimmond, B. J.; Corey, J. Y. *Organometallics* **1999**, *18*, 2223. (b) Grimmond, B. J.; Corey, J. Y.; Rath, N. P. *Organometallics* **1999**, *18*, 404.

(9) Although achiral catalysts would intrinsically be expected to provide atactic polyolefins, the ability of achiral metallocenes to generate polyolefins with some degree of stereoregularity via a chain-end control mechanism has been demonstrated. Ewen, J. A. *J. Am. Chem. Soc.* **1984**, *106*, 6355−6364.

(10) Nonrigid catalysts that were subject to rapid exchange between achiral and chiral forms have been shown to generate polypropylene with varying degrees of isotacticity. (a) Tagge, C. D.; Kravchenko, R. L.; Lal, T. K.; Waymouth, R. M. *Organometallics* **1999**, *18*, 380. (b) Coates, G. W.; Waymouth, R. M. *Science* **1995**, *267*, 217.

(11) Grimmond, B. J.; Corey, J. Y. *Organometallics* **1999**, *18*, 4646.

(12) Lofthus, O. W.; Slebodnick, C.; Deck, P. A. *Organometallics* **1999**, *18*, 3702.

presence of one $^{29}Si$ environment and reaffirming the time-averaged $C_2$-symmetric nature of compound **3**. The complete assignment of these resonances in both **3** and **4** was made in conjunction with $^1H-^1H$ COSY, $^1H-^{13}C\{^1H\}$ HETCOR, and $^1H-^1H$ NOE studies.

The monosubstituted enantiopure siloxy-functionalized metallocene dichlorides $Cp(Cp^{Si*})MCl_2$ (M = Ti, **5**; Zr, **6**) were also synthesized by salt elimination methods (eq 3). Compound **5** was prepared from **2** and $CpTiCl_3$

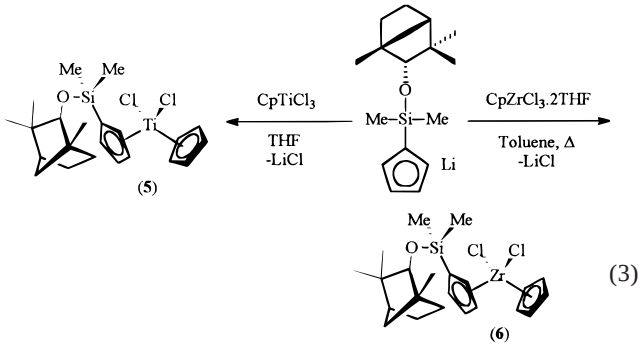


(3)

in THF. The red solid formed after removal of the solvent was recrystallized from $CH_2Cl_2$/pentane and was sublimed to give analytically pure **5** in moderate yield. The corresponding zirconocene **6** was obtained from a 1:1 mixture of **2** and $CpZrCl_3 \cdot 2THF$ in toluene. Filtration of the reaction mixture through Celite afforded a clear yellow solution of **6**, from which the volatiles were removed in vacuo. Sublimation of the residue provided analytically pure **6** as a white powder in excellent yield (77%). Compounds **5** and **6** were characterized as $C_1$-symmetric metallocene dichlorides by $^1H$, $^{13}C\{^1H\}$, and $^{29}Si\{^1H\}$ NMR spectroscopy in a manner similar to that described for **3** and **4**. A series of $^1H-^1H$ COSY, $^1H-^{13}C\{^1H\}$ HETCOR, and $^1H-^1H$ NOE techniques were then used to fully assign the resonances observed.

Upon purification, metallocene dichlorides **3**−**6** were soluble in common chlorinated, ethereal, and aromatic solvents, while being partially soluble in hydrocarbon solvents such as pentanes. Although compounds **3**−**6** could be manipulated in air in the solid state, prolonged exposure of solutions of **3**−**6** to the atmosphere resulted in gradual decomposition.

**Solid State Analysis of 6.** White needlelike crystals of the monosubstituted zirconocene dichloride **6** were obtained by recrystallization from an $Et_2O$/pentanes solution. An X-ray diffraction study of these crystals established that **6** was an asymmetric siloxy-substituted zirconocene dichloride, in good agreement with the solution state evidence provided by NMR spectroscopy. Compound **6** crystallized in a monoclinic unit cell and refined satisfactorily in the noncentrosymmetric space group $P2(1)$. The absolute stereochemistry of the (1*R*)-*endo*-(+)-fenchol substituent was confirmed. An ORTEP plot of **6** is presented in Figure 2, with relevant collection data and selected geometric parameters provided in Tables 1 and 2, respectively. The geometry of the Zr metal center with respect to the two chloride ligands and the Cp and $Cp^{Si*}$ centroids is pseudotetrahedral, and bond lengths and angles of **6** are in reasonable agreement with those of other previously determined monosubstituted zirconocene dichlorides.[14] The $SiMe_2$ substituent projects from the Cp ring with the two methyl groups pointing toward the metal center.

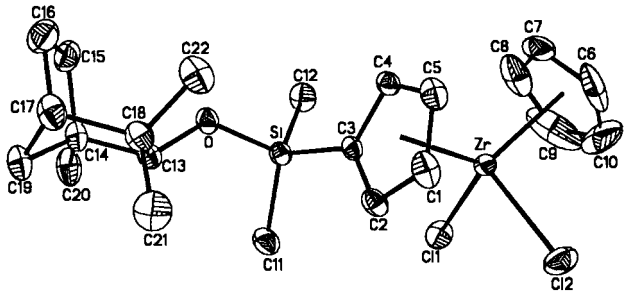


**Figure 2.** ORTEP plot of $Cp(Cp^{Si*})ZrCl_2$, **6**, with 50% probability ellipsoids. The hydrogen atoms have been omitted for clarity.

**Table 1. Crystal Structure Data and Structure Refinement of $Cp(Cp^{Si*})ZrCl_2$**

| | |
|---|---|
| empirical formula | $C_{22}H_{32}Cl_2OSiZr$ |
| fw | 502.69 |
| temperature | 213(2) K |
| wavelength | 0.71073 Å |
| cryst syst | monoclinic |
| space group | $P2_1$ |
| unit cell dimens | $a = 6.5560(1)$ Å<br>$b = 25.3561(3)$ Å, $\beta = 112.291(1)°$<br>$c = 7.6815(1)$ Å |
| volume | 1181.50(3) Å$^3$ |
| $Z$ | 2 |
| density (calcd) | 1.413 Mg/m$^3$ |
| abs coeff | 0.752 mm$^{-1}$ |
| $F(000)$ | 520 |
| cryst size | 0.22 × 0.10 × 0.04 mm$^3$ |
| $\theta$ range for data collection | 1.61−26.41° |
| index ranges | $-8 \le h \le 7$,<br>$-31 \le k \le 31$,<br>$-9 \le l \le 9$ |
| no. of reflns collected | 15 937 |
| no. of ind reflns | 4836 [$R$(int) = 0.056] |
| completeness to $\theta = 26.41°$ | 99.9% |
| abs corr | empirical |
| max. and min. transmsn | 0.9705 and 0.8521 |
| refinement method | full-matrix least-squares on $F^2$ |
| no. of data/restraints/params | 4836/11/244 |
| goodness-of-fit on $F^2$ | 1.047 |
| final $R$ indices [$I>2\sigma(I)$] | R1 = 0.0343, wR2 = 0.0671 |
| $R$ indices (all data) | R1 = 0.0468, wR2 = 0.0720 |
| absolute structure param | −0.02(4) |
| largest diff peak and hole | 0.245 and −0.285 e Å$^{-3}$ |

**Table 2. Selected Bond Lengths [Å] and Angles [deg] for $Cp(Cp^{Si*})ZrCl_2$**

| | | | |
|---|---|---|---|
| Zr−Cl(1) | 2.4443(10) | Cl(1)−Zr−Cl(2) | 97.15(4) |
| Zr−Cl(2) | 2.4541(10) | O−Si−C(11) | 110.33(17) |
| Zr−C(1) | 2.519(4) | O−Si−C(12) | 105.15(17) |
| Zr−C(2) | 2.526(4) | C(11)−Si−C(12) | 113.4(2) |
| Zr−C(3) | 2.535(4) | O−Si−C(3) | 106.60(15) |
| Zr−C(4) | 2.478(4) | C(11)−Si−C(3) | 111.64(19) |
| Zr−C(5) | 2.485(4) | C(12)−Si−C(3) | 109.35(18) |
| Si−O | 1.642(3) | C(13)−O−Si | 128.5(2) |
| Si−C(11) | 1.851(4) | C(5)−C(1)−C(2) | 107.9(4) |
| Si−C(12) | 1.857(4) | C(1)−C(2)−C(3) | 108.8(4) |
| Si−C(3) | 1.881(4) | C(4)−C(3)−C(2) | 106.1(3) |
| O−C(13) | 1.426(4) | C(3)−C(4)−C(5) | 108.9(4) |
| C(1)−C(5) | 1.381(6) | C(1)−C(5)−C(4) | 108.2(4) |
| C(1)−C(2) | 1.413(5) | O−C(13)−C(14) | 111.1(3) |
| C(2)−C(3) | 1.417(6) | O−C(13)−C(18) | 115.0(3) |
| C(3)−C(4) | 1.407(5) | | |
| C(4)−C(5) | 1.413(6) | | |

(13) Mitchell, J. P.; Hajela, S.; Brookhart, S. K.; Hardcastle, K. I.; Henling, L. M.; Bercaw, J. E. *J. Am. Chem. Soc.* **1996**, *118*, 1045−1053.

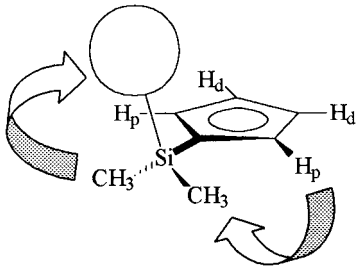


**Figure 3.** Illustration of $^1H-^1H$ NOE contacts observed for $Cp(Cp^{Si*})ZrCl_2$, **6**. Strong correlations from the neighboring fenchoxy methyl protons (H-20, H-21) to the alkoxy proton (H-13) were obtained. Further through-space contacts between the $SiMe_2$ protons (H-11,12) to H-13 and to proximal Cp protons ($H_p$, H-2,4) were noted. This series of NOE contacts suggested that the chiral nature of the fenchol ligand was relayed to the Cp ancillary ligand via the $SiMe_2$ group.

Consequently the remaining fenchoxy substituent is oriented over the $Cp^{Si*}$ ring such that it lies on the $Cp^{Si*}$ face opposite that of the $\eta^5$-$\pi$-bound metal center. Presumably, this arrangement in the solid state minimized the steric interactions throughout the molecule, with special attention toward avoiding steric contacts between the fenchoxy substituent and the $ZrCl_2$ metal core. The C(2)−C(3)−Si−C(11) dihedral angle of −27.7° staggers the three Si substituents with respect to the C(1)−C(5) $Cp^{Si*}$ ring plane. This is further illustrated by the C(4)−C(3)−Si−C(12) dihedral angle of 38.9°, which prevents an eclipsed alignment of the silyl methyl groups C(11) and C(12) with the adjacent $Cp^{Si*}$ ring (bonds C(3)−C(2) and C(3)−C(4) in Figure 2) and thereby minimizes any steric interaction between the two.

**Correlation of $^1H-^1H$ NOE Contacts to Nonbonded Distances.** The resonances for the four inequivalent proximal and distal protons of **6** were distinguished by $^1H-^1H$ NOE spectroscopy. As shown in Figure 3, NOE contacts were observed exclusively from the $SiMe_2$ protons to only two of the four $Cp^{Si*}$ protons. These correlations were assumed to exist between the $SiMe_2$ protons and the nearby proximal $Cp^{Si*}$ protons, given the inverse correlation between NOE intensity and $^1H-^1H$ nonbonded distance. This was verified by closer inspection of the solid state structure of **6**, where the nonbonded distances of the proximal $Cp^{Si*}$ protons [attached to C(2) and C(4) in Figure 3] to the $SiMe_2$ methyl protons [of C(11) and C(12)] ranged from 3.75 to 4.78 Å, with an average of 4.28 Å. However, the nonbonded distances from the methyl groups to the distal protons were significantly longer, at 5.11−5.67 Å, with an average of 5.40 Å. This would tend to explain why NOE contacts were observed exclusively between the nearby methyl protons and the proximal protons in the $^1H-^1H$ NOE spectrum and not to the remote distal protons. It should be noted that the siloxy ligand rotates about the Si−C(3) bond in solution. For this reason, the nonbonded distances obtained from the solid state structure are not constantly maintained in solution. However, the solid state data do provide a reasonable illustration of the typical nonbonded distances in solution. Minor NOE contacts from the unsubstituted ring to the $SiMe_2$ protons were also observed. In the solid state, the shortest nonbonded distances between the $SiMe_2$ protons and the $C_5H_5$ protons ranged from 3.09 to 4.69 Å; however, the remaining nonbonded distances were greater than 5.00 Å.

**Table 3. Molecular Weight Data from the Polymerization Studies of $PhSiH_3$**

| catalyst[a] | $M_w$[b] | $M_n$[b] | PDI[b] | $D_p$[c] | L:C[b] |
|---|---|---|---|---|---|
| $Cp_2TiCl_2$ | 1500 | 1000 | 1.5 | 13 | 1.3 |
| $Cp_2ZrCl_2$ | 2000 | 1000 | 2.0 | 13 | 1.8 |
| $Cp(Cp^{Si*})TiCl_2$ | 1900 | 1100 | 1.7 | 14 | 1.0 |
| $Cp(Cp^{Si*})ZrCl_2$ | 2100 | 1600 | 1.3 | 20 | 2.0 |
| $(Cp^{Si*})_2ZrCl_2$ | 4100 | 2400 | 1.7 | 31 | 9.0 |

[a] 1.0 mol % catalyst activated with 2.0 mol % *n*-BuLi. Reactions were run at ambient temperature (25 °C) for 48 h. [b] Measured by GPC analysis of the PPSi samples. PDI = $M_w/M_n$. L:C = ratio of linear/cyclic products in sample. [c] The degree of polymerization was calculated from $D_p = (M_n/104)2[r(C)/r(Si)]$. $r$ = appropriate atomic radii.

**$PhSiH_3$ Dehydropolymerization Studies with Asymmetric Metallocenes 3−6.** The chiral metallocene dichlorides were investigated as catalysts for the dehydropolymerization of $PhSiH_3$ to PPSi. As shown in eq 4, 1.0 mol % of the metallocene dichlorides was

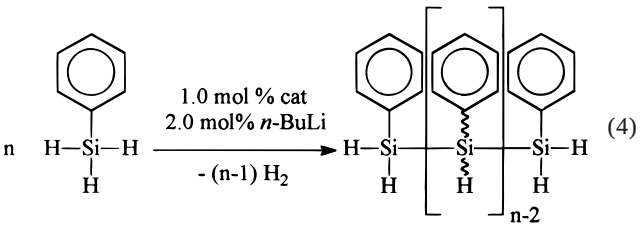


(4)

cat. $Cp(Cp^{Si*})MCl_2$ (M = Ti, Zr), $(Cp^{Si*})_2ZrCl_2$

activated by combination with 2.0 mol % of *n*-BuLi in neat, degassed $PhSiH_3$. The Hf compound **4** was not activated under these conditions; limited or minor dehydropolymerization activity has been observed for previously investigated hafnocene systems.[15] After 48 h, the material obtained was dissolved in THF and filtered through Celite to separate the catalyst residues. Removal of the solvent in vacuo provided each PPSi sample as a gum-like material whose molecular weight properties were determined by GPC analysis.

As shown in Table 3, the $M_w$ properties of each polymerisate were dependent on the metallocene catalyst used. In comparison with the appropriate parent metallocene [$Cp_2MCl_2$/2 *n*-BuLi M = Ti, Zr] under the same conditions, the siloxy-substituted metallocenes generated PPSi with higher average $M_w$ values. With regard to the degree of substitution of the Cp rings, progressive substitution appeared to elevate the $M_w$ values consistent with trends observed in previously studied metallocene catalysts.[16] Additionally, Ti-based catalysts produced lower $M_w$ PPSi samples when compared to the analogous Zr system. The degree of PPSi polymerization relied on the ratio of high $M_w$ linear PPSi (LPPSi) to low $M_w$ oligocyclic PPSi (CPPSi) generated. When catalysts produced lesser quantities of the CPPSi and larger quantities of LPPSi, the average molecular values of the net sample increased. Generally, Zr-based

(14) Cardin, D. J.; Lappert, M. F.; Raston, C. L. *Chemistry of Organo-Zirconium and Organo-Hafnium Compounds*; John Wiley and Sons: New York, 1986.

(15) Shaltout, R. M.; Corey, J. Y. *Main Group Chem.* **1995**, *1*, 115.
(16) Imori, T.; Tilley, T. D. *Polyhedron* **1994**, *13*, 1548.

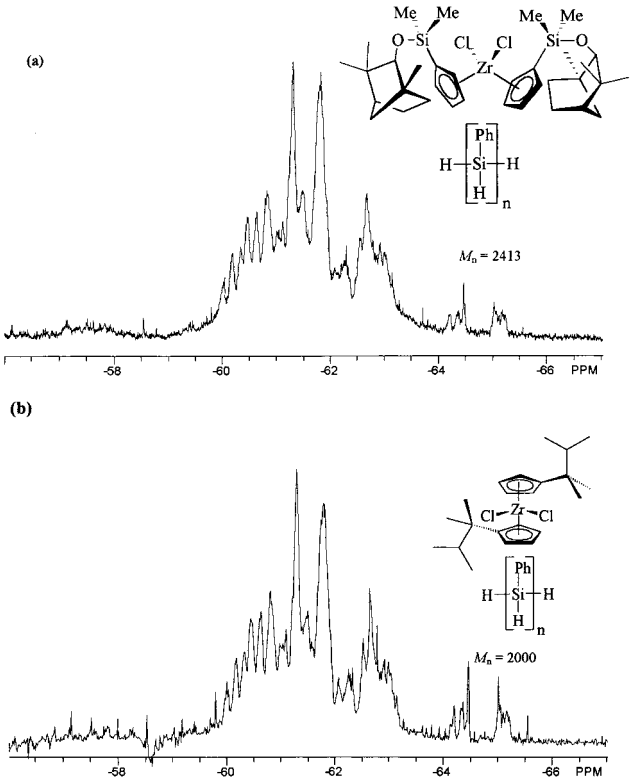


**Figure 4.** $^{29}Si\{^1H\}$ DEPT spectrum ($C_6D_6$, 303 K, 500 MHz) of LPPSi using the heteroannular disubstituted precatalysts (a) $(Cp^{Si*})_2ZrCl_2$ and (b) $Cp^R)_2ZrCl_2$.

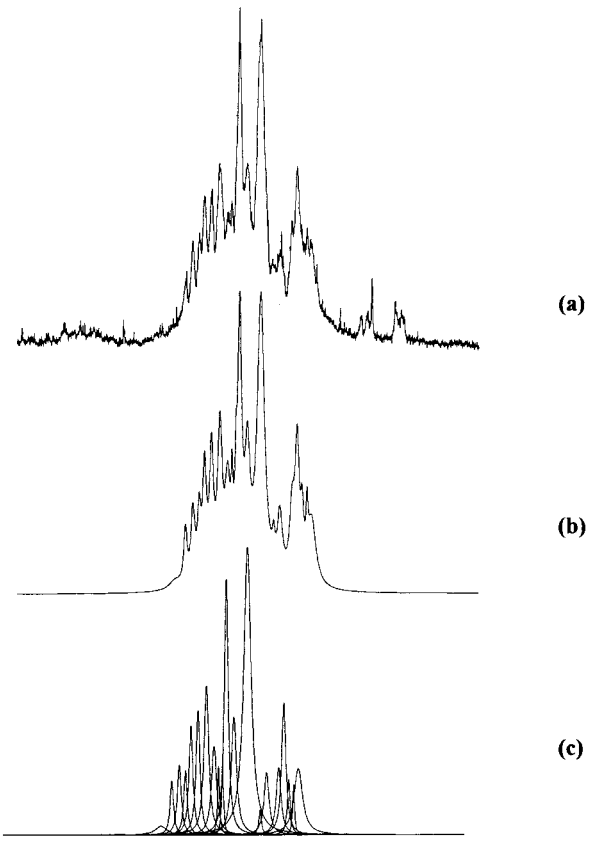


**Figure 5.** Stacked plot of (a) $^{29}Si\{^1H\}$ DEPT data for the LPPSi produced using $(Cp^{Si*})_2ZrCl_2$ as the precatalyst; (b) simulated spectrum; (c) deconvolution peaks of simulation.

catalysts produced the least amount of CPPSi. Additionally, progressive substitution of the Cp rings, i.e., Cp vs $Cp(Cp^{Si*})$ vs $(Cp^{Si*})_2$, consecutively suppressed CPPSi formation and thereby increased the PPSi average $M_w$ values by producing greater amounts of LPPSi.

**LPPSi Stereochemistry.** The asymmetric zirconocene $(Cp^{Si*})_2ZrCl_2$, **3**, produced predominantly (90%) LPPSi with the highest $M_w$ (4100), as established by GPC. This sample was therefore suitable for microstructure analysis by $^{29}Si\{^1H\}$ NMR spectroscopy because it contained mostly higher order linear silicon chains. A $C_6D_6$ $^{29}Si\{^1H\}$ NMR spectrum of the LPPSi sample revealed the polymer microstructure to be atactic. This was evaluated first by comparison with the $^{29}Si\{^1H\}$ NMR spectrum of an authentic *a*-LPPSi sample of comparable $M_w$ value which had been generated under similar conditions using the achiral zirconocene precatalyst $[CpC(CH_3)_2CH(CH_3)_2]_2ZrCl_2$ (Figure 4). As shown in Figure 4, the general features of the two spectra appeared to be very similar, suggesting that the polymers were likely to have similar stereochemical characteristics. On closer inspection of the chemical shift region ($\delta = -59.75$ to $-63.02$ ppm) that corresponded to the tertiary internal P(Ph*Si*H)P′ silicon centers (P/P′ = inequvalent polymer segements), the degree of stereoregularity could be more accurately determined. The LPPSi spectrum in Figure 4a was duplicated to within 1.0% error by deconvolution techniques using a collection of 20 deconvolution peaks (Figure 5). The intensity of each chemical shift region that corresponded to the previously assigned rr, mr, and mm triad stereodomains was then established by summation of the individual deconvolution peaks within each region.[8a] The results of the deconvolution study are summarized in Table 4. The 0.30 (rr):0.51 (mr):0.19 (mm) ratio of the net intensities of the triad stereodomains was the expected distribution for an atactic or nearly atactic polysilane sample (*a*-LPPSi), under a Bernoullian statistical model. With the probabilty of a meso stereoreplication of 45% (Pm = 0.45), the predicted distribution of triad intensities was 0.30 (rr):0.50 (mr):0.20 (mm), in good agreement with the actual data obtained. This result indicated that the LPPSi sample produced from the asymmetric zirconocene dichloride $(Cp^{Si*})_2ZrCl_2$ was effectively atactic (*a*-LPPSi). For the PPSi sample obtained from the precatalyst $Cp(Cp^{Si*})ZrCl_2$, **6**, the larger amount of oligocyclic materials tended to overly complicate the $^{29}Si\{^1H\}$ spectrum and prevented a similar analysis. However, the broad, poorly defined nature of the spectrum suggested that the PPSi sample obtained from **6** was also atactic (*a*-PPSi).

**Table 4. Triad Assignments and Peak Intensity Ratios of *a*-LPPSi**

| triad entry | chemical shift range (ppm) | parent peak intensity[a–c] | unit ratio | Bernoullian predicted ratio | (Pm)-(1 − Pm) |
|---|---|---|---|---|---|
| rr | −59.75/−60.82 | 160.348 | 0.30 | 0.30 | 0.45 0.55 |
| mr | −61.00/−62.26 | 270.120 | 0.51 | 0.50 | |
| mm | −62.55/−63.02 | 102.687 | 0.19 | 0.20 | |

[a] The values above were generated when the four variable peaks were included as mr type resonances. [b] Parent peak range (intensity): rr: −59.75/−60.82 (160.35). mr: −61.207/−61.796 (202.41). mm: −62.55/−63.02 (102.69). A complete list of deconvolution peak chemical shifts and intensities are supplied in the Supporting Information. [c] Variable peaks (intensity): (a) −61.00 (24.58), (b) −61.11 (18.99), (c) −62.10 (6.94), (d) −62.257 (17.207).

## Discussion

**Precatalyst Synthesis and Reactivity.** The chiral siloxy-functionalized metallocene dichlorides $(Cp^{Si*})_2MCl_2$ (M = Zr, **3**; Hf, **4**) and $Cp(Cp^{Si*})MCl_2$ (M = Ti, **5**; Zr, **6**) were synthesized in variable yield by salt metathesis reactions of the lithium salt **2** and the appropriate metal halide synthon. For those metathesis reactions carried out in THF, the yields were significantly reduced in comparison to the metallocene dichlorides obtained by a similar salt elimination reaction in toluene. The metallocene dichlorides obtained in toluene required further purification by sublimation. On prolonged exposure to atmospheric conditions, solutions of the siloxy-functionalized metallocenes hydrolyzed to produce the corresponding bimetallic disiloxane, as shown in eq 5. Presumably, this occurred by the hydrolysis of the $Cp^{Si*}$ ligand to fenchol and the silanol intermediate, which then dimerized via a condensation reaction, as has been reported for a related $Fc_2Si(OH)_2$ system (Fc = $(C_5H_5)_2Fe$).[17] The nature of the final decomposition product was unambiguously established by X-ray crystallographic analysis of the bimetallic disiloxane $[CpTiCl_2C_5H_4SiMe_2]_2O$ obtained from a solution of **5** on prolonged atmospheric exposure.[18]

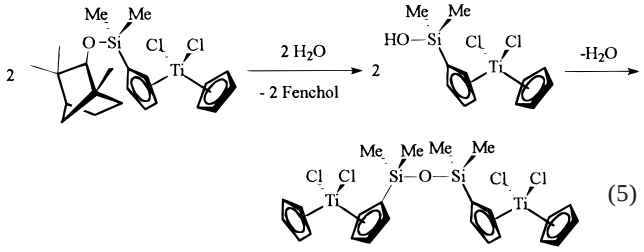


**Catalyst Structural Selection**. The monosubstituted and the heteroannular disubstituted metallocene dichlorides **3**−**6** all possessed a chiral enantiopure fenchoxy ligand. This rendered the compounds chiral and thus potentially capable of influencing the chemistry that takes place at the metal center involving the generation of a new stereocenter. Typically, $C_2$-symmetric chiral ansa-metallocenes are used as catalysts to induce the formation of highly stereoregular polyolefins from prochiral olefin monomers.[6,19] The rigid nature of the chiral ansa-catalyst frame is believed to be a major contributor to the high degree of stereoreplication. The analogous non-ansa-metallocenes produced polyolefins with variable degrees of stereoregularity due to the free rotation of the functionalized ancillary Cp ligands. Despite this factor, it was elected to first investigate the non-ansa chiral metallocenes **3**−**6** for reasons of structural simplicity and primarily due to the fact that sila-bridged ansa-metallocenes have been shown to produce only oligomeric polyphenylsilane.[15] The ethano-linked ansa-metallocenes $(EBTHI)MCl_2$ [M = Ti, Zr; EBTHI = 1,2-bis(3-tetrahydroindenyl)ethane] have also been employed as $PhSiH_3$ dehydropolymerization catalysts in combination with a cocatalyst.[20,21] However, the Ti derivative was ineffective for producing polymers from $PhSiH_3$.[21] Additionally, separation of oligocyclic PPSi was necessary when using Zr-based catalysts. The current interpretation of the PPSi $^{29}Si\{^1H\}$ spectra obtained is that the polymers are atactic, indicating that the ansa-metallocenes failed to direct the stereochemistry of the PPSi chain by enantiomorphic site control.[21]

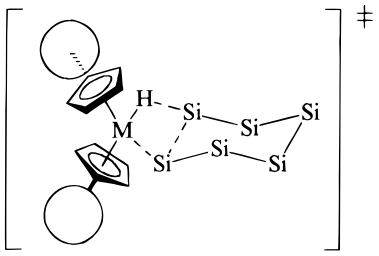


**Figure 6.** Proposed $\sigma$-bond metathesis transition state which leads to cyclization of hexasilyl unit to produce cyclic-$Ph_6Si_6H_6$ and a metal hydride. The silyl substituents (Ph, H) have been omitted for clarity.

**Influence of $Cp^{Si*}$ Functionalization on PPSi $M_w$ Properties.** The molecular weight properties of the PPSi obtained were dictated by the catalyst selection. Generally, Ti-based catalysts gave PPSi samples with a lower average degree of polymerization in comparison to the Zr analogues. Additionally, progressive siloxy substitution of the metallocene structure increased the $M_w$ of the PPSi sample in part by inhibiting the formation of low $M_w$ CPPSi. Thus, the $PhSiH_3$ polymerization using the catalyst $(Cp^{Si*})_2ZrCl_2$/2 *n*-BuLi gave the LPPSi sample of highest $M_w$ (4100) with lowest CPPSi content (10%). In agreement with this observation, the substitution of the Cp ring with bulky achiral groups in other metallocenes has been previously shown to impede the formation of oligocyclic silanes.[8] This behavior can be attributed to the $\sigma$-bond metathesis[22] mechanism, which is commonly believed to account for the stepwise propagation of PPSi. Under this mechanism, the cyclization of the oligomeric chains ideally occurs by the key folding of a $\sigma$-bound hexasilyl ligand ($Si_6$) or related oligomeric ligand ($Si_4$, $Si_5$, $Si_7$) back toward the metal hydride center $Ph_6Si_6H_7$−M−H (Figure 6). A $\sigma$-bond metathesis transition state as shown in Figure 6 then generates a metal hydride M−H, with the concomitant cyclization and expulsion of the hexasilyl moiety c-$Ph_6Si_6H_6$. The use of the $Cp^{Si*}$ ligand instead of the unsubstituted Cp ring appears to block the path of the hexasilyl unit to the metal center and thereby suppresses extensive cyclization.

High-performance metallocene catalysts are easily capable of producing polyolefins with $M_w > 10^5$, whereas similar catalysts struggle to produce PPSi with $M_w > 10^3$. This disparity can be traced to the different

(17) Maclachlan, M. J.; Zhang, J.; Manners, I.; Mordas, C.; LeJuer, R.; Geiger, W. E.; Liable-Sands, L. M.; Rheingold, A. L. *Organometallics* **1999**, *18*, 1337.

(18) (a) Grimmond, B. J.; Corey, J. Y.; Rath, N. P. *Acta Crystallogr.* **2000**, *C56*, 53. (b) Noh, S. K.; Byun, G.-G.; Lee, S.-S.; Yoon, K.-B.; Kang, K. S. *J. Organomet. Chem.* **1996**, *518*, 1

(19) (a) Ewen, J. A.; Haspeslagh, L.; Atwood, J. L.; Zhang, H. M. *J. Am. Chem. Soc.* **1987**, *109*, 6544−6545. (b) Wild, F. R. W. P.; Zsolnai, L.; Hutter, G.; Brintzinger, H.-H. *J. Organomet. Chem.* **1982**, *232*, 233.

(20) Banovetz, J. P.; Stein, K.; Waymouth, R. *Organometallics* **1991**, *10*, 3430.

(21) Dioumaev, V. K.; Rahimian, K.; Gauvin, F.; Harrod, J. F. *Organometallics* **1999**, *18*, 2249.

(22) (a) Woo, H.-G.; Walzer, J. F.; Tilley, T. D. *J. Am. Chem. Soc.* **1992**, *114*, 7047. (b) Woo, H.-G.; Heyn, R. H.; Tilley, T. D. *J. Am. Chem. Soc.* **1992**, *114*, 5698 (c) Woo, H.-G.; Tilley, T. D. *J. Am. Chem. Soc.* **1989**, *111*, 3757. (d) Woo, H.-G.; Tilley, T. D. *J. Am. Chem. Soc.* **1989**, *111*, 8043.

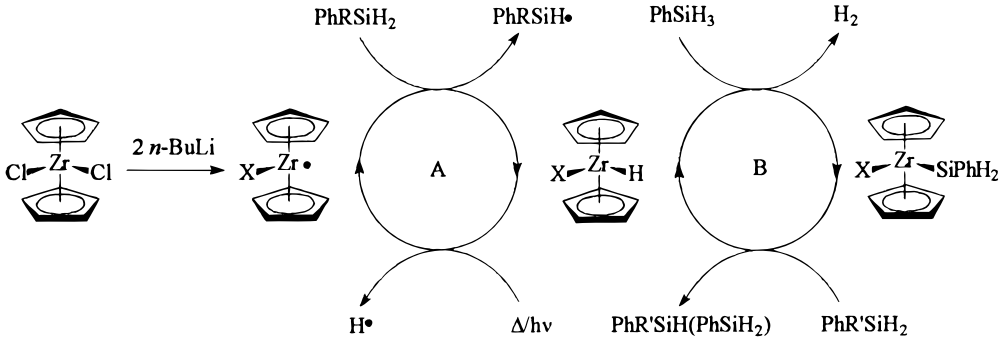


**Figure 7.** Simplified scheme showing dehydrocoupling through a radical route (A) and through $\sigma$-bond metathesis (B). X may be a group such as H, Bu, or an organic substituent or may be no substituent. R or R′ may be H or the polymer chain.



mechanisms by which propagation of the polymer takes place. Olefin polymerization occurs by a chain-growth mechanism with insertion of the monomer substrate into a metal−alkyl polymer bond. This process requires a moderate degree of net monomer consumption before polymers of significant size are created at the catalyst site. On the other hand, the step-growth dehydropolymerization of silanes to polysilanes requires that effectively all of the monomer or low-order oligomer feed be consumed before coupling to higher order oligomers and polymers may take place. It is likely that an alternative process will have to be established for the efficient manufacturing of higher order polysilanes ($M_w \approx 10^4$) by dehydrocoupling.

**Influence of $Cp^{Si*}$ Functionalization on PPSi Stereochemistry.** A sample of higher order LPPSi was obtained when using the $C_2$-symmetric chiral zirconocene **3** as a catalyst. The metallocene $(Cp^{Si*})_2ZrCl_2$ was the most likely to produce stereoregular LPPSi due to the presence of two bulky enantiopure functional groups and the time-averaged $C_2$ symmetry of the catalyst. The fact that hindered zirconocene-based catalysts, such as **3**, produce predominantly LPPSi suggested that the Cp ligand substituents influenced the polymer growth. Furthermore, the observation of NOE contacts from the $SiMe_2$ protons to the chiral fenchol unit and to the Cp protons suggested that chiral information could be efficiently relayed throughout the entire catalyst framework. It therefore seemed reasonable to assume that this chiral environment would effect substrates, such as silanes, that were bound to the metal center and direct some degree of stereobias for any transformation that occurred at the metal center. Indeed, (*R*,*R*)-(EBTHI)$TiF_2$ and *S*,*S*,*S*-(EBTHI)Ti(binaphtholate)/RLi have both been utilized in the hydrosilylation of prochiral ketones producing alcohols with modest to excellent ee's.[23] Thus, for the metallocene-catalyzed propagation of LPPSi, a partially stereoregular polysilane would be predicted. However, the combination system $(Cp^{Si*})_2ZrCl_2$/2 *n*-BuLi was ineffective as a catalyst for the stereocontrolled growth of LPPSi according to NMR spectroscopic evidence. The $^{29}Si\{^1H\}$ NMR spectrum indicated that the LPPSi was effectively atactic, with a 0.30 (rr):0.50 (mr):0.20 (mm) ratio of the triad stereodomains, which corresponded to a meso replication probability Pm = 0.45. These data demonstrated that the current catalyst candidate was incapable of LPPSi stereocontrol, producing only *a*-LPPSi similar to that observed for all other achiral group 4 metallocene-based catalysts. Given the success of similar strategies in stereoregular olefin polymerization technology, it is somewhat surprising that chiral metallocenes fail to generate PPSi without even a moderate degree of stereobias. There are several possibilities that could explain this observation including a non-metal-mediated (radical) coupling during the stereodetermining step or a metal-mediated process where there is insufficient interaction of the prochiral polysilane Ph(P)$SiH_2$ end group (P = polymer) with the chiral metallocene envelope.

Harrod and co-workers have previously proposed that a radical dehydrocoupling process may account for the lack of stereocontrol of LPPSi when chiral metallocenes are employed.[21] The combination of $Cp_2ZrCl_2$ and *n*-BuLi provides $Cp_2ZrBu_2$, which undergoes one-electron reduction at room temperature to give a mixture of approximately 50% Zr(III) and 50% Zr(IV) by NMR and EPR spectroscopic analysis.[24] The addition of $B(C_6F_5)_3$ to $Cp'_2ZrCl_2$/*n*-BuLi/$PhSiH_3$ (Cp′ = $C_5H_5$ or substituted derivative) produces a cationic metal complex that enhances the molecular weight of the polysilane product. A one-electron oxidative addition−reductive elimination mechanism producing silyl radicals was proposed for this catalyst system, and it was coupling of silicon radicals that formed the polysilane product.[25] Consequently the PPSi chain would propagate outside the vicinity of the metal center. Under a radical regime, the stereochemical nature of the catalyst, i.e., chiral or achiral, would have no effect on the stereogrowth of the LPPSi, thereby accounting for the observed formation of *a*-LPPSi. In support of this suggestion, Harrod et al. reported only *a*-LPPSi when using the chiral catalysts [EBTHI]Ti(*S*,*S*-BINOL)/2 *n*-BuLi, [EBTHI]$MCl_2$, and [EBI]$MCl_2$ (EBI = 1,2-bis(3-indenyl)ethane; M = Ti, Zr).[21] A similar radical mechanism could explain the *a*-LPPSi obtained from the chiral precatalyst $(Cp^{Si*})_2ZrCl_2$ with *n*-BuLi. A related decomposition of $(Cp^{Si*})_2ZrBu_2$ to $(Cp^{Si*})_2ZrBu$ or the highly reactive $(Cp^{Si*})_2Zr$ species[26b,c] would provide a possible entry into a radical dehydropolymerization scheme (Figure 7, cycle A). The

(23) (a) Rahimian, K.; Harrod, J. F. *Inorg. Chim. Acta* **1998**, *270*, 330. (b) Yun, J.; Buchwald, S. L. *J. Am. Chem. Soc.* **1999**, *121*, 5640.

(24) Dioumaev, V. K.; Harrod, J. F. *Organometallics* **1997**, *16*, 1452.

(25) Dioumaev, V. K.; Harrod, J. F. *J. Organomet. Chem.* **1996**, *521*, 133.

(26) Radicals have been reported previously from group 4 complexes. (a) Tumas, W.; Wheeler, D. R.; Grubbs, R. H. *J. Am. Chem. Soc.* **1987**, *109*, 6182. (b) Eisch, J. J.; Owuor, F. A.; Shi, X. *Organometallics* **1999**, *18*, 1583. (c) Eisch, J. J.; Shi, X.; Owuor, F. A. *Organometallics* **1998**, *17*, 5219.

simplified pathway presented in Figure 7 illustrates a situation wherein the metal center serves to merely extract a hydrogen radical from a silicon center producing a silyl radical. Coupling of silyl radicals then produces the polysilane.

It is also possible that the *a*-LPPSi propagation occurs by a $\sigma$-bond metathesis route (Figure 7, cycle B) but without efficient stereocontrol of the polysilane chain. In the initial approach of $PhPSiH_2$ (P = polymer) to $(Cp^{Si*})_2Zr(SiPhH_2)$, the selection of which prochiral Si−H bond is activated by the metal center would be determined by the interactions of the remaining Si substituents (Ph/P) with the chiral metallocene structure. Since the atomic radius of Si is relative large (1.17 Å[27]), the distance between the end group Ph/P substituents and the ancillary metallocene ligands could be such that the catalyst cannot effectively discriminate between the prochiral Si−H protons of the terminal silicon center on the basis of the minor steric interactions between the catalyst and the remote substituents. Thus, the catalyst may only recognize two large substituents that cannot be distinguished in the vicinity of the prochiral Si center. The general outcome would lead to diastereomeric $\sigma$-bond metathesis transition states of similar free energies, the nonselective activation of the prochiral Si−H bonds during the $\sigma$-bond metathesis step, and ultimately *a*-LPPSi.

## Conclusion

A series of chiral group 4 siloxy-functionalized metallocene dichlorides $(Cp^{Si*})_2MCl_2$ (M = Zr, **3**; Hf, **4**) and $Cp(Cp^{Si*})MCl_2$ (M = Ti, **5**; Zr, **6**) were synthesized and characterized by standard methods. When combined with 2 equiv of *n*-BuLi, the compounds were active catalysts for the dehydropolymerization of $PhSiH_3$ to a mixture of oligocyclic and linear polyphenylsilane (PPSi). The highest $M_w$ LPPSi samples were obtained when using the heteroannular disubstituted zirconocene dichloride **3** as a precatalyst. A $^{29}Si\{^1H\}$ NMR spectrum of the LPPSi obtained when using **3** as a catalyst revealed that the polysilane was predominantly atactic (*a*-LPPSi, Pm = 0.45), which indicated that the chiral catalyst did not direct the regulation of the stereogrowth of the LPPSi via an enantiomorphic site control mechanism.

## Experimental Section

**General Comments**. All reactions were run under an atmosphere of dry nitrogen using Schlenk glassware and techniques unless otherwise stated. Reaction vessels were flame dried under a stream of nitrogen, and anhydrous solvents were transferred by oven-dried syringes or cannula. Tetrahydrofuran was distilled from calcium hydride and then from sodium benzophenone ketyl; diethyl ether was distilled from sodium benzophenone ketyl. Toluene, pentanes, and hexanes were distilled from calcium hydride, and dichloromethane was washed with sulfuric acid, neutralized, and distilled from calcium hydride.

Microanalyses were performed by Atlantic Microlab, Inc., Norcross, GA.

Proton and carbon-13 ($^1H$, $^{13}C$) nuclear magnetic resonance spectra were recorded using either a Varian Unity + 300 equipped with a multinuclear probe or a Bruker ARX500 equipped with a broad band or inverse probe. Two-dimensional NMR spectroscopy studies were performed using a Bruker ARX500. Unless otherwise stated, spectra were recorded in $CDCl_3$ and referenced internally to residual solvent peaks ($CHCl_3$) or to TMS. Chemical shifts ($\delta$) are reported in ppm and coupling constants (*J*) in hertz. $^1H$ NMR used for accurate determination of signal ratios was run with a delay of 0.5−1.0 s to minimize the effects of differential relaxation periods. The labeling of the $^1H$ and $^{13}C\{^1H\}$ resonances of **3**−**6** follows the scheme illustrated in Figure 8. The reagents *n*-BuLi, $ZrCl_4$, and $HfCl_4$ (Aldrich) were used as received. The starting materials $PhSiH_3$, $ZrCl_4$·2THF, $HfCl_4$·2THF,[28] $CpZrCl_3$·2THF,[29] $CpTiCl_3$,[30] and compound **1**[11] were prepared according to literature procedures.

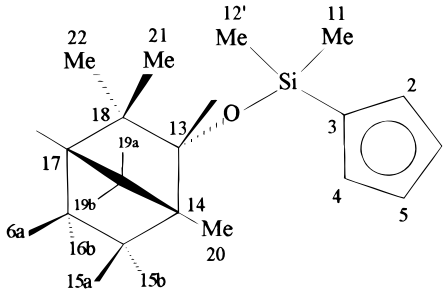


**Figure 8.** Numbering key for spectroscopic assignments.

After polymerization experiments were completed, the catalysts were deactivated by exposure to air. An aliquot was extracted and dissolved in freshly distilled THF, and the solution was passed by syringe through a 6000 series nonsterile 0.45 m PTFE filter before obtaining GPC measurements. GPC data were collected using an SSI 222D HPLC pump to elute the samples through a bank of $10^4$ Å, $10^2$ Å, and 500 Å Waters 78 × 300 mm Ultrastyragel columns in HPLC grade THF solvent. Detection of the polymers was carried out using a Linear UV−vis detector set to 254 nm. The silicon-29 ($^{29}Si$) nuclear magnetic resonance spectra were recorded using a Bruker ARX500 equipped with a broad band probe. Unless otherwise stated, polymer $^1H$ spectra were recorded in $C_6D_6$ and referenced internally to the residual solvent peak ($C_6H_6$). The $^{29}Si\{^1H\}$ DEPT spectra were also recorded in $C_6D_6$ and referenced externally. Unequal NOE suppression or enhancement of signal intensities was assumed to be negligible, as established by Schilling, Bovey, and Zeigler for $^{29}Si$ signals of polysilanes.[31] Deconvolution of the $^{29}Si\{^1H\}$ DEPT spectrum was carried out using a NMR Utility Transform Software (NUTS) package from Acorn NMR.

**Synthesis of $LiC_5H_4SiMe_2(1R)$-*endo*-(+)-$OC_{10}H_{17}$ (2).** A sample of $C_5H_5SiMe_2(1R)$-endo-(+)-$OC_{10}H_{17}$ (**1**) (12.75 g, 46.2 mmol) was dissolved in $Et_2O$ (50 mL) to give a colorless solution, which was cooled to 0 °C. On adding *n*-BuLi (18.5 mL, 46.2 mmol) dropwise over 10 min, a white precipitate was obtained. The reaction mixture was allowed to stir for 2 h with gradual warming to room temperature. The resultant white precipitate was isolated by filtration and washed with $Et_2O$ (40 mL). Drying the residue in vacuo afforded **2** as a white solid (12.82 g, 98% yield).

**Synthesis of $(C_5H_4SiMe_2(1R)$-*endo*-(+)-$OC_{10}H_{17})_2ZrCl_2$ (3).** A Schlenk tube was charged with samples of **2** (1.00 g, 3.5 mmol) and $ZrCl_4$·2THF (0.64 g, 1.7 mmol) in a glovebox. The Schlenk tube was transferred to a Schlenk line and evacuated for 10 min. After backflushing with $N_2$, toluene (35 mL) was introduced by syringe to provide a thick suspension. The reaction mixture was heated to 80 °C for 48 h with stirring

(27) Pauling, L. *The Nature of the Chemical Bond*, 3rd ed.; Cornell University Press: Ithaca, NY, 1960; p 260.

(28) Manzer, L. E. *Inorg. Synth.* **1982**, *21*, 135.
(29) Lund E. C.; Livinghouse, T. *Organometallics* **1990**, *9*, 2426.
(30) Cardoso, A. M.; Clark, R. J. H. Moorhouse, S. J. *J. Chem. Soc., Dalton Trans.* **1980**, 1156.
(31) Schilling, F. C.; Bovey, F. A.; Zeigler, J. M. *Macromolecules* **1986**, *19*, 2309.

to afford a yellow solution and a fine suspension. After cooling to ambient temperature, the reaction mixture was filtered through Celite and the Celite pad was washed with toluene (3 × 5 mL). The clear toluene filtrates were combined and the volatiles removed in vacuo to give an off-white solid. Sublimation (180 °C, 1 mTorr) of the solid gave **3** as a white powder (0.73 g, 60% yield). $^1$H NMR: 6.80 (m, 2H, Cp-H-2,4), 6.59 (q, $J$ = 2.6 Hz, 1 H, Cp-H-1,5), 6.55 (q, $J$ = 2.6 Hz, 1 H, Cp-H-1,5), 3.24 (d, $J$ = 1.5 Hz, 1 H, H-13), 1.82 (m, 1H, H-15), 1.68 (m, 2 H, H-16, H-17), 1.40 (m, 1 H, H-19a), 1.39 (m, 1 H, H-16), 1.10 (dd, $J$ = 10.0, 1.3 Hz, 1 H, H-19b), 0.96 (s, 3 H, H-22), 0.89 (m, 1 H, H-15), 0.88 (s, 3 H, H-21), 0.77 (s, 3 H, H-20), 0.40 (s, 6 H, Si−$CH_3$-11,12). $^{13}$C{$^1$H} NMR: 125.6, 125.4 (Cp-2,4), 121.3 (ipso-Cp-3), 116.5, 115.9 (Cp-1,5), 86.12 (C-13), 49.70 (C-14), 48.54 (C-17), 41.10 (C-19) 39.60 (C-18), 30.56 (C-22), 26.40 (C-16), 25.82 (C-15), 21.55 (C-21), 20.16 (C-20), 0.66, 0.16 (Si−$CH_3$-11,12). $^{29}$Si{$^1$H} NMR: 2.51 (s). Anal. Calcd for $C_{34}H_{54}O_2ZrCl_2$: C, 57.27; H, 7.63. Found: C, 56.70; H, 7.46.

**Synthesis of ($C_5H_4SiMe_2$(1*R*)-*endo*-(+)-$OC_{10}H_{17}$)$_2HfCl_2$ (4).** A Schlenk tube was charged with samples of **2** (1.00 g, 3.5 mmol) and $HfCl_4$·2THF (0.79 g, 1.7 mmol) in a glovebox. The Schlenk tube was transferred to a Schlenk line, evacuated for 10 min, and cooled to −78 °C. After backflushing with $N_2$, THF (15 mL) was introduced by syringe to provide an orange solution, which was stirred for 12 h with gradual warming to room temperature. An orange solution containing a fine precipitate was obtained, and the volatiles were then removed in vacuo. The reaction vessel was removed to a glovebox and the reaction mixture transferred to a Soxhlet extractor. The apparatus was transferred to a Schlenk line, evacuated for 10 min, and backfilled with $N_2$. Extraction with $CH_2Cl_2$ (20 mL) provided a clear brown solution, which was reduced to ∼5 mL and layered with pentanes (5 mL). Storage at −50 °C prompted the precipitation of an off-white solid, which was recrystallized from $CH_2Cl_2$/pentanes (1:1) at −50 °C. The resultant white solid was isolated by syringe filtration and dried in vacuo to afford **4**·$CH_2Cl_2$ as a white powder (0.16 g, 12% yield). $^1$H NMR: 6.80 (m, 2H, Cp-H-2,4), 6.57 (q, $J$ = 2.6 Hz, 1 H, Cp-H-1,5), 6.54 (q, $J$ = 2.6 Hz, 1 H, Cp-H-1,5), 3.22 (d, $J$ = 1.5 Hz, 1 H, H-13), 1.78 (m, 1H, H-15), 1.67 (m, 2 H, H-16, H-17), 1.41 (m, 1 H, H-19a), 1.38 (m, 1 H, H-16), 1.07 (dd, $J$ = 10.0, 1.3 Hz, 1 H, H-19b), 0.94 (s, 3 H, H-22), 0.89 (m, 1 H, H-15), 0.86 (s, 3 H, H-21), 0.79 (s, 3 H, H-20), 0.40 (s, 6 H, Si−$CH_3$-11,12). $^{13}$C{$^1$H} NMR: 126.6, 126.0 (Cp-2,4), 123.61 (ispo-Cp-3), 117.8, 117.2 (Cp-1,5), 86.07 (C-13), 49.67 (C-14), 48.47 (C-17), 41.05 (C-19) 39.57 (C-18), 30.53 (C-22), 26.38 (C-16), 25.77 (C-15), 21.54 (C-21), 20.16 (C-20), 0.61, 0.12 (Si−$CH_3$-11,12). $^{29}$Si{$^1$H} NMR: 2.61 (s). Anal. Calcd for $C_{35}H_{56}O_2Si_2HfCl_4$: C, 47.48; H, 6.37. Found: C, 47.44; H, 6.50.

**Synthesis of $C_5H_5$($C_5H_4SiMe_2$(1*R*)-*endo*-(+)-$OC_{10}H_{17}$)$TiCl_2$ (5).** A Schlenk tube was charged with samples of (**2**) (0.42 g, 1.5 mmol) and $CpTiCl_3$ (0.33 g, 1.5 mmol) in a glovebox. The Schlenk tube was transferred to a Schlenk line, evacuated for 10 min, and cooled to −78 °C. After backflushing with $N_2$, THF (15 mL) was introduced by syringe to give a yellow solution, which was stirred for 12 h with gradual warming to room temperature. A red solution with a fine precipitate was obtained, and the volatiles were removed in vacuo. The Schlenk tube was transferred to a glovebox and the reaction mixture transferred to a Soxhlet extractor. The apparatus was then returned to a Schlenk line, evacuated for 10 min, and backfilled with $N_2$. Extraction with $CH_2Cl_2$ (20 mL) provided a clear red solution, which was reduced in volume to ∼5 mL and layered with pentanes (5 mL). Storage at −50 °C gave a red solid, which was isolated by syringe filtration and dried in vacuo. The red solid was sublimed (160 °C, 1 mTorr) to give **4** as red powder (0.26 g, 38% yield). $^1$H NMR: 6.63 (m, 1H, Cp-H-2,4), 6.60 (m, 1 H, Cp-H-2,4), 6.12 (s, 5 H, $C_5H_5$), 6.02 (q, $J$ = 2.6 Hz, 2 H, Cp-H-1,5), 3.20 (d, $J$ = 1.6 Hz, 1 H, H-13), 1.93 (m, 1H, H-15), 1.72 (m, 1 H, H-16), 1.60 (m, 1H, H-17), 1.38 (m, 1 H, H-16), 1.34 (m, 1 H, H-19a), 1.02 (dd, $J$ = 10.2, 1.4 Hz, 1 H, H-19b), 0.96 (m, 1H, H-15), 0.96 (s, 3 H, H-20), 0.86 (s, 3 H, H-21), 0.85 (s, 3 H, H-22), 0.45 (s, 3 H, Si−$CH_3$-11,12), 0.45 (s, 3 H, Si−$CH_3$-11,12). $^{13}$C{$^1$H} NMR: 129.8, 129.1 (Cp-2,4), 120.6, 120.2 (Cp-1,5), 120.1 ($C_5H_5$), 87.17 (C-13), 50.12 (C-14), 49.03 (C-17), 41.42 (C-19) 40.00 (C-18), 30.86 (C-22), 26.93 (C-16), 26.32 (C-15), 21.99 (C-21), 20.54 (C-20), 0.66, 0.24 (Si−$CH_3$-11,12). The *ipso*-Cp carbon was not located. $^{29}$Si{$^1$H} NMR: 3.45 (s). Anal. Calcd for $C_{22}H_{32}OSiTiCl_2$: C, 57.52; H, 7.02. Found: C, 57.11; H, 6.90.

**Synthesis of $C_5H_5$($C_5H_4SiMe_2$(1*R*)-*endo*-(+)-$OC_{10}H_{17}$)$ZrCl_2$ (6).** A Schlenk tube was charged with samples of (**2**) (0.62 g, 2.5 mmol) and $CpZrCl_3$·2THF (1.00 g, 2.5 mmol) in a glovebox. The Schlenk tube was transferred to a Schlenk line and evacuated for 10 min. After backflushing with $N_2$, toluene (50 mL) was introduced by syringe to provide a thick suspension. The reaction mixture was heated to 50 °C for 24 h with stirring to afford a yellow solution and a fine suspension. After cooling to ambient temperature, the reaction mixture was filtered through Celite and the Celite pad was washed with toluene (2 × 10 mL). The clear yellow toluene filtrates were combined and the volatiles removed in vacuo to give an off-white solid. Sublimation (150 °C, 1 mTorr) of the solid provided **6** as a white powder (0.95 g, 77% yield). $^1$H NMR ($C_6D_6$): 6.50 (t, $J$ = 2.6 Hz, 2H, Cp-H-2,4), 6.00 (q, $J$ = 2.6 Hz, 1 H, Cp-H-1,5), 5.98 (q, $J$ = 2.6 Hz, 1 H, Cp-H-1,5), 6.04 (s, 5 H, $C_5H_5$), 3.17 (d, $J$ = 1.7 Hz, 1 H, H-13), 1.95 (m, 1H, H-15), 1.72 (m, 1 H, H-16), 1.59 (m, 1H, H-17), 1.37 (m, 1 H, H-16), 1.34 (m, 1 H, H-19a), 1.00 (dd, $J$ = 10.0, 1.5 Hz, 1 H, H-19b), 0.96 (m, 1H, H-15), 0.96 (s, 3 H, H-20), 0.85 (s, 3 H, H-21), 0.83 (s, 3 H, H-22), 0.47 (s, 3 H, Si−$CH_3$-11,12), 0.46 (s, 3 H, Si−$CH_3$-11,-12). $^{13}$C{$^1$H} NMR ($C_6D_6$): 126.2, 125.7 (Cp-2,4), 124.2 (Cp-ipso-3), 117.6, 117.3 (Cp-1,5), 116.4 ($C_5H_5$), 86.19 (C-13), 50.04 (C-14), 48.97 (C-17), 41.32 (C-19), 40.00 (C-18), 30.90 (C-22), 26.86 (C-16), 26.22 (C-15), 21.97 (C-21), 20.48 (C-20), 0.78, 0.39 (Si−$CH_3$-11,12). $^{29}$Si{$^1$H} NMR ($C_6D_6$): 2.60 (s). Anal. Calcd for $C_{22}H_{32}OSiZrCl_2$: C, 52.56; H, 6.42. Found: C, 52.82; H, 6.49.

**Polymerization Studies**. In a glovebox, a Schlenk tube was charged with $(Cp^{Si*})_2ZrCl_2$ (0.03 g, 4.35 × $10^{-2}$ mmol) and transferred to a Schlenk line, where it was evacuated and backfilled with $N_2$. A sample of $PhSiH_3$ (0.47 g, 4.35 mmol) was added by syringe, and the colorless reaction mixture was degassed by three freeze−pump−thaw cycles. At ambient temperature, the catalyst was activated on addition of *n*-BuLi (0.02 mL, 2.5 M), resulting in the evolution of a gas and the formation of a yellow-orange solution. The reaction mixture was stirred for 48 h, to provide a viscous yellow gum, which was dissolved in THF and filtered through Celite. The solvent was removed in vacuo to provide the polysilane as an off-white gum (yield 0.37 g, 80%).

**X-ray Structural Determination**. Colorless, needle-shaped crystals of **6** were grown from a 1:1 mixture of $Et_2O$/pentanes at −35 °C over a period of two months. A crystal with dimensions 0.22 × 0.10 × 0.04 mm$^3$ was mounted on glass fibers in a random orientation. Preliminary examination and data collection was performed using a Bruker SMART charge coupled device (CCD) detector system single-crystal X-ray diffractometer using graphite-monochromated Mo Kα radiation ($\lambda$ = 0.71073 Å) equipped with a sealed tube X-ray source at −60 °C. Preliminary unit cell constants were determined with a set of 45 narrow frames (0.3° in $\omega$) scans. A typical data set collected consists of 4028 frames of intensity data collected with a frame width of 0.3° in $\omega$ and counting time of 15 s/frame at a crystal-to-detector distance of 4.930 cm. The double pass method of scanning was used to exclude any noise. The collected frames were integrated using an orientation matrix determined from the narrow frame scans. SMART and SAINT software packages (Bruker Analytical X-ray, Madison, WI, 1998) were used for data collection and data integration. Analysis of the integrated data did not show any decay. Final cell constants were determined by a global refinement of *xyz*

centroids of 6791 reflections ($\theta < 26°$). Collected data were corrected for systematic errors using SADABS[32] based on the Laue symmetry using equivalent reflections. The integration process yielded 15 937 reflections, of which 4836 ($2\theta < 52.8°$) were independent reflections.

Crystal data and intensity data collection parameters are listed in Table 1.

Structure solution and refinement were carried out using the SHELXTL- PLUS software package (Sheldrick, G. M., Bruker Analytical X-Ray Division, Madison, WI, 1999). The structure was solved by direct methods and refined successfully in the space group $P2_1$. Full matrix least-squares refinement was carried out by minimizing $\sum w(F_o^2 - F_c^2)^2$. The non-hydrogen atoms were refined anisotropically to convergence. The hydrogen atoms were treated using an appropriate riding model (AFIX m3). One of the Cp rings (C6−C10) exhibits rotational disorder, which could not be resolved. Geometrical constraints (SADI, SHELX-TL) were used for the refinement of this disordered Cp ring. The final residual values were $R(F) = 3.43\%$ for 4221 observed reflections [$I > 2\sigma(I)$] and $wR(F^2) = 7.20\%$; $s = 1.05$ for all data. The absolute structure was determined using Flack's parameter (Flack $x = -0.02(4)$).[33]

(32) Blessing, R. H. *Acta Crystallogr.* **1995**, *A51*, 33.
(33) Flack, H. D. *Acta Crystallogr.* **1983**, *A39*, 876.

Structure refinement parameters are listed in Table 1. The atomic coordinates for the non-hydrogen atoms and the geometrical parameters are listed in Tables S1 and S2, respectively. A projection view of the molecule with non-hydrogen atoms represented by 50% probability ellipsoids and showing the atom labeling is presented in Figure 1.

Complete listings of positional and isotropic displacement coefficients for hydrogen atoms and anisotropic displacement coefficients for the non-hydrogen atoms are submitted as Supporting Information. Tables of calculated and observed structure factors are available in electronic format.

**Acknowledgment.** Funding from the UM Research Board, a UMSL Research Award, and a Mallinckrodt Fellowship for B.J.G. are gratefully acknowledged. We also thank Dr. J. Braddock-Wilking for helpful discussions.

**Supporting Information Available:** Tables of crystal structure data and refinement details, atomic coordinates and equivalent isotropic parameters, and hydrogen coordinates and isotropic displacement parameters for **6**. This material is available free of charge via the Internet at http://pubs.acs.org.

OM0002935